Diagnostic and Interventional Imaging 102 (2021) 735–742

Original article/*Abdominal imaging*

Enhancing capsule in hepatocellular carcinoma: intra-individual comparison between CT and MRI with extracellular contrast agent

Roberto Cannella[a,b,c], Maxime Ronot[a,d], Riccardo Sartoris[a,d], Francois Cauchy[e], Christian Hobeika[e], Aurélie Beaufrere[f], Loïc Trapani[f], Valérie Paradis[f], Mohamed Bouattour[g], Fanny Bonvalet[a], Valérie Vilgrain[a,d], Marco Dioguardi Burgio[a,d,*]

[a] *Department of Radiology, AP-HP.Nord, Hôpital Beaujon, 92110 Clichy, France*
[b] *Section of Radiology - BiND, University Hospital "Paolo Giaccone", 90127 Palermo, Italy*
[c] *Department of Health Promotion Sciences Maternal and Infant Care, Internal Medicine and Medical Specialties, PROMISE, University of Palermo, 90127 Palermo, Italy*
[d] *Université de Paris, Faculté de Médecine & INSERM U1149 "centre de recherche sur l'inflammation", CRI, F-75018 Paris, France*
[e] *Department of HPB Surgery and Liver Transplantation, AP-HP.Nord, Hôpital Beaujon, 92110 Clichy, France*
[f] *Department of Pathology, AP-HP.Nord, Hôpital Beaujon, 92110 Clichy, France*
[g] *Department of Digestive Oncology, AP-HP.Nord, Hôpital Beaujon, 92110 Clichy, France*

ARTICLE INFO

Keywords:
Capsule
Computed tomography
Extracellular contrast agent
Hepatocellular carcinoma
Magnetic resonance imaging

ABSTRACT

Purpose: The purpose of this study was to compare the value of contrast-enhanced computed tomography (CT) to that of magnetic resonance imaging obtained with extracellular contrast agent (ECA-MRI) for the diagnosis of a tumor capsule in hepatocellular carcinoma (HCC) using histopathologic findings as the standard of reference.

Materials and methods: This retrospective study included patients with pathologically-proven resected HCCs with available preoperative contrast-enhanced CT and ECA-MRI examinations. Two blinded radiologists independently reviewed contrast-enhanced CT and ECA-MRI examinations to assess the presence of an enhancing capsule. The histopathological analysis of resected specimens was used as reference for the diagnosis of a tumor capsule. The sensitivity and specificity of CT and ECA-MRI for the diagnosis of a tumor capsule were determined, and an intra-individual comparison of imaging modalities was performed using McNemar test. Inter-reader agreement was assessed using Kappa test.

Results: The study population included 199 patients (157 men, 42 women; mean age: 61.3 ± 13.0 [SD] years) with 210 HCCs (mean size 56.7 ± 43.7 [SD] mm). A tumor capsule was present in 157/210 (74.8%) HCCs at histopathologic analysis. Capsule enhancement was more frequently visualized on ECA-MRI (R1, 68.6%; R2, 71.9%) than on CT (R1, 44.3%, $P < 0.001$; R2, 47.6%, $P < 0.001$). The sensitivity of ECA-MRI was better for the diagnosis of histopathological tumor capsule (R1, 76.4%; R2, 79.6%; $P < 0.001$), while CT had a greater specificity (R1, 84.9%; R2, 83.0%; $P < 0.001$). Inter-reader agreement was moderate both on CT (kappa = 0.55; 95% confidence interval [CI]: 0.43–0.66) and ECA-MRI (kappa = 0.57; 95% CI: 0.45–0.70).

Conclusion: Capsule enhancement was more frequently visualized on ECA-MRI than on CT. The sensitivity of ECA-MRI was greater than that of CT, but the specificity of CT was better than that of ECA-MRI.

1. Introduction

Hepatocellular carcinoma (HCC) is the most common primary liver malignancy, representing about 90% of all liver malignancies in patients with cirrhosis [1]. In patients with a high pre-test probability of HCC, the diagnosis of HCC can be achieved noninvasively in lesions larger than 10 mm on multiphase contrast-enhanced computed tomography (CT) and magnetic resonance imaging (MRI) based on typical imaging features including hyperenhancement during the hepatic arterial phase and nonperipheral washout on subsequent vascular phases [1]. These features reflect microscopic vascular changes that occur during hepatocarcinogenesis [2,3].

Besides these changes, HCC often also results in the formation of a peripheral tumor capsule corresponding to various amounts of peritumoral fibrous tissue, prominent sinusoids, or compressed liver parenchyma on histopathological examination [4]. On imaging, this capsule presents as a peripheral enhancing rim on portal venous and

Abbreviations: CI, Confidence interval; CT, Computed tomography; ECA-MRI, MRI with extracellular contrast agent; HCC, Hepatocellular Carcinoma; LI-RADS, Liver Imaging Reporting and Data System; MRI, Magnetic resonance imaging; SD, Standard deviation

* Corresponding author at: Department of Radiology, AP-HP.Nord, Hôpital Beaujon, 100 Boulevard du Général Leclerc, 92110 Clichy, France.
E-mail address: marco.dioguardiburgio@aphp.fr (M. Dioguardi Burgio).

https://doi.org/10.1016/j.diii.2021.06.004
2211-5684/

delayed phases and is referred to as an "enhancing capsule" [4]. The specificity of this "enhancing capsule" ranges between 89 and 100% for the diagnosis of HCC, justifying its inclusion in the Liver Imaging Reporting and Data System (LI-RADS) algorithm as a major imaging feature [5–9]. In LI-RADS v2018, the presence of enhancing capsule is sufficient to categorize ≥ 20 mm lesions with nonrim arterial phase hyperenhancement as definitively HCC (LR-5) [9], even in the absence of other major imaging features (*i.e.*, nonperipheral washout or threshold growth). However, the performance of imaging for the detection of enhancing capsule may vary according to the imaging technique and the type of contrast agent.

Prior studies evaluating the imaging appearance of HCC with different imaging modalities and contrast agents reported a greater prevalence of enhancing capsule on contrast-enhanced CT than on gadoxetate disodium-enhanced MRI [10], and also on MRI obtained with extracellular contrast agents (ECA-MRI) by comparison with MRI obtained with gadoxetate disodium [11–15]. This is probably due to the different pharmacokinetics of gadolinium-based contrast agents. The accurate diagnosis of tumor capsule is relevant for patient prognostication as it is associated with prolonged progression-free survival after surgical resection [16,17]. However, no prior study has reported the intraindividual comparison of CT and ECA-MRI for the diagnosis of a tumor capsule. We hypothesize that visualization of enhancing capsule could differ between CT and ECA-MRI because of the different spatial and contrast resolution of the two modalities.

The purpose of this study was to compare the value of CT to that of ECA-MRI for the diagnosis of a tumor capsule in HCC using histopathologic findings as the standard of reference.

2. Materials and methods

This retrospective study was approved by the local IRB (CRM-2103-131), and patient informed consent was waived due to the retrospective design.

2.1. Population

A search for the pathology records was performed between 2012 and 2019 to select adult patients with pathologically-proven HCC following hepatic resection and with available preoperative contrast-enhanced CT and ECA-MRI examinations. The initial population included 308 patients (239 men, 69 women) with a mean age of 61.7 ± 12.7 (standard deviation [SD]) years who underwent resection for HCC. Exclusion criteria were as follows: (*i*), multiple (≥ 3) resected HCCs preventing a reliable radiological-pathological correlation (n = 24); (*ii*), HCC treated before preoperative imaging (n = 4); and (*iii*), lack of preoperative contrast-enhanced CT (n = 29) or ECA-MRI (n = 52) examinations. For patients with multiple preoperative imaging studies, the CT and MRI examinations performed before treatment and closest to the date of surgery were selected as index examinations. Fig. 1 shows the flow-chart of the study.

Patient-related variables including sex, age, etiology of underlying chronic liver disease, and date of surgery were retrieved using the electronic data systems.

2.2. Imaging technique

All patients underwent multiphase contrast-enhanced CT and ECA-MRI according to the most recent liver protocols. CT and MRI examinations were acquired with different scanners due to the retrospective study design. Patients were given a weight-based dose of intravenous iodinated contrast agent for contrast-enhanced CT, with an iodine concentration of 350 g/L, injected with a power injector at a rate of 3–4 mL/s. Contrast-enhanced MRI sequences were acquired after intravenous administration of a gadolinium-based extracellular contrast agent (Gd-BOPTA, Gadobenate Dimeglumine, MultiHance®, Bracco Imaging; Gd-DOTA, gadoterate meglumine, Dotarem®, Guerbet; or occasionally other gadolinium-based extracellular contrast agents), injected with a power injector at a rate of 2 mL/s. Post-contrast images included late hepatic arterial (acquired with bolus triggering technique), portal venous (70–90 s), and delayed (180 s) phases.

2.3. Imaging analysis

Two radiologists blinded to the results of histopathological analysis (R1, M.D.B., and R2, R.C., with 10- and 6 years of experience in abdominal and liver imaging, respectively), independently reviewed all imaging studies on the picture archiving and communication system (Vue PACS, Philips Healthcare). CT and MRI examinations were reviewed independently and in random order to minimize recall bias. The readers assessed lesion size and the presence of enhancing capsule on CT and MRI examinations. Lesion size was recorded as the largest diameter on either axial, coronal, or sagittal planes measured from outer edge to outer edge of the lesions and including the enhancing capsule [9]. The enhancing capsule was characterized according to the definition in the CT/MRI LI-RADS v2018 algorithm: "smooth, uniform, sharp border around most or all of an observation, unequivocally thicker or more conspicuous than fibrotic tissue around background nodules, and visible as an enhancing rim in portal venous or delayed phases" [9].

To assess the added value of the identification of enhancing capsule for the diagnosis of HCC in the subset of patients corresponding to the high-risk population in LI-RADS v2018, readers assigned a category to each tumor using the LI-RADS v2018 algorithm with and without considering enhancing capsule as a major feature [9].

2.4. Reference standard

The reference standard for the HCC capsule was based on a histopathological analysis of resected specimens. All histopathological specimens were reviewed by an expert pathologist (A.B.) with 8 years' experience in liver pathology. The presence of a capsule was first assessed macroscopically then confirmed by the microscopic examination. An encapsulated HCC nodule was defined by the presence of fibrous tissue surrounding the nodule and separating it from the adjacent liver parenchyma. Microscopically, the capsule was considered to be complete when it totally surrounded the nodule and incomplete when it surrounded at least one third of its circumference. Both microscopically complete and incomplete capsules were considered for the purpose of this study.

Non-tumoral liver parenchyma from resected specimens was evaluated to assess the stage of fibrosis and presence of hepatic steatosis. Liver fibrosis was graded as follows: F0, no fibrosis; F1, portal fibrosis without septa; F2, portal fibrosis with rare septa; F3, numerous septa without cirrhosis; and F4, cirrhosis [18]. Patients with non-tumoral liver parenchyma assigned to F3-F4 were considered to have advanced fibrosis. Steatosis was considered present when involving at least 5% of the hepatocytes.

2.5. Statistical analysis

Categorical variables were expressed as raw numbers, proportions and percentages, while continuous variables were reported as means ± SD and ranges. Categorical variables were compared using the Chi-square (χ^2) or Fisher exact test. Intraindividual differences between CT and MRI examinations were assessed using the McNemar test for categorical variables and Wilcoxon signed rank-sum test for continuous variables. Sensitivity, specificity, and accuracy with their 95% confidence intervals (CIs) were calculated for the diagnosis of a macroscopic and microscopic capsule at histopathology. Corresponding true positive, true negative, false positive, false negative and proportions were provided. Sensitivities, specificities, and accuracies

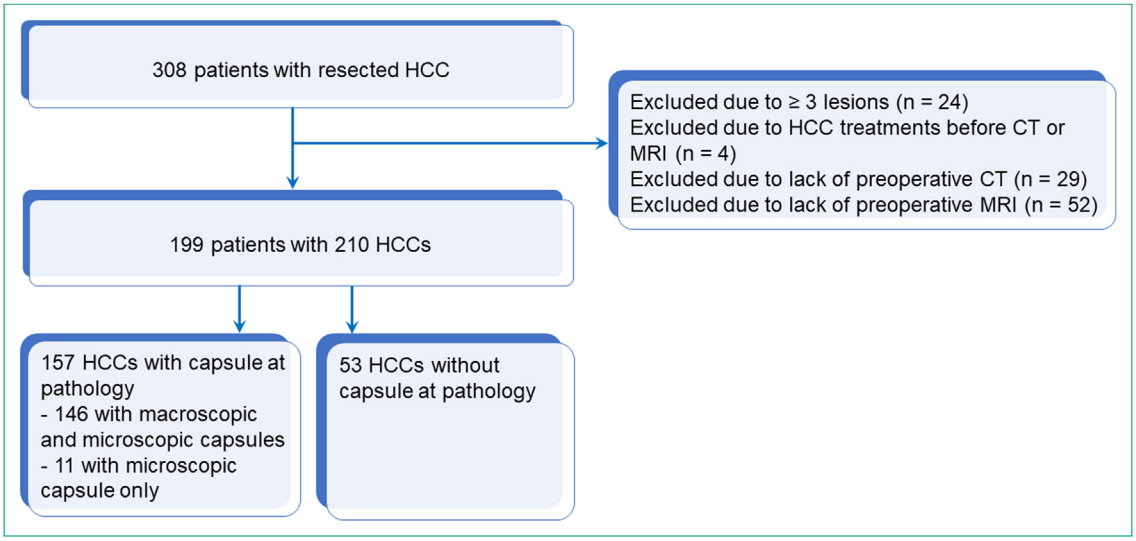

Fig. 1. Flowchart of the study population. HCC: hepatocellular carcinoma.

derived from CT and MRI were also compared using the McNemar test.

The Cohen's kappa (k) test was used to assess inter-reader agreement. Agreement was categorized as poor (k < 0.00), slight (k = 0.00 −0.20), fair (k = 0.21−0.40), moderate (k = 0.41−0.60), substantial (k = 0.61−0.80), or almost perfect (k = 0.81−1.00) [19].

P < 0.05 was considered to be statistically significant. Statistical analyses were performed using SPSS Software (Version 20.0. Armonk, NY, USA: IBM Corp).

3. Results

3.1. Population and tumors

The characteristics of the final population are summarized in Table 1. The final population included 199 patients (157 men, 42 women) with a mean age of 61.3 ± 13.0 [SD] years (age range: 21 −89 years) with 210 pathologically-proven HCCs (mean size 56.7 ± 43.7 [SD] mm; range: 8−241 mm). Among them, 188/199 (94.5%) patients had a single HCC and 11/199 (5.5%) patients had two HCCs. Overall 66/210 (31.4%) HCCs measured < 30 mm (including 33 lesions < 20 mm), 59/210 (28.1%) measured 30−49 mm, and 85/210 (40.5%) were ≥ 50 mm.

Table 1
Characteristics of the study population.

Characteristics	Number (%)
Patients	199
Sex	
Male	157 (157/199; 78.9%)
Female	42 (42/199; 21.1%)
Age (years)	61.3 ± 13.0 [21−89]
Etiology of chronic liver disease	
Hepatitis C	32 (32/199; 16.1%)
Hepatitis C + alcohol or NAFLD	18 (18/199; 9.0%)
Hepatitis B	46 (46/199; 23.1%)
Hepatitis B + alcohol or NAFLD	9 (9/199; 4.5%)
Nonalcoholic fatty liver disease	49 (49/199; 24.7%)
Alcohol	12 (12/199; 6.0%)
Others	10 (10/199; 5.0%)
No chronic liver disease	23 (23/199; 11.6%)
*Hepatic fibrosis stage**	
F0	18 (18/199; 9.0%)
F1	30 (30/199; 15.1%)
F2	41 (41/199; 20.6%)
F3	44 (44/199; 22.1%)
F4	66 (66/199; 33.2%)

Categorical variables are expressed as raw numbers; numbers in parentheses are proportions followed by percentages; continuous variables are expressed as means ± standard deviation; numbers in bracket are ranges.
Abbreviation. NAFLD: nonalcoholic fatty liver disease.
* Fibrosis staging was performed using METAVIR scoring system.

3.2. Tumor capsule at pathology

Tumor capsule was observed in 157/210 (74.8%) HCCs on histopathology (microscopic capsule without a macroscopic capsule only being observed in 11 HCCs). A tumor capsule was observed in 41/66 (62.1%), 50/59 (84.7%), and 66/85 (77.6%) HCCs < 30 mm, 3−49 mm and ≥ 50 mm (P = 0.011), respectively. Microscopically, HCC capsule was considered to be complete in 102 (46.4%) tumors and incomplete in 55 (25.0%).

3.3. Performance of imaging for the diagnosis of tumor capsule

The mean time between index CT and MRI examinations and surgical resection was 66.7 ± 87.4 (SD) days (range: 0−259 days) and 88.5 ± 96.5 (SD) days (range: 1−290 days) (P < 0.001), respectively. The interval between CT and MRI examinations was 46.2 ± 54.6 (SD) days (range: 0−280 days).

The prevalence of enhancing capsules identified with both modalities are reported in Table 2. Enhancing capsule was identified significantly more frequently on ECA-MRI than on contrast-enhanced CT by both readers (P < 0.001 for both R1 and R2) and was observed in 93/210 (44.3%, R1) and 100/210 (47.6%, R2) HCCs on contrast-enhanced CT and in 144/210 (68.6%, R1) and 151/210 (71.9%, R2) HCCs on ECA-MRI, respectively (Figs. 2 and 3). Subgroup analysis according to the size of HCCs confirmed that enhancing capsule was significantly more frequently visualized on ECA-MRI in all subgroups (R1, P = 0.004; R2, P < 0.001 in HCC < 30 mm; P = 0.001 for both R1 and R2 in HCC measuring 30−49 mm; and R1, P < 0.001; R2, P = 0.001 in HCCs ≥ 50 mm).

The diagnostic performances of contrast-enhanced CT and ECA-MRI for the diagnosis of tumor capsule are presented in Table 3. The sensitivity of ECA-MRI was significantly geater than that of contrast-enhanced CT for the diagnosis of tumor capsule (R1, 76.4% *vs.* 54.1%, P < 0.001; R2, 79.6% *vs.* 57.9%, P < 0.001), which was confirmed in all tumor size subgroups. The specificity of contrast-enhanced CT was significantly greater than that of ECA-MRI for the diagnosis of tumor

Table 2
Visibility of enhancing capsule on contrast-enhanced CT and MRI with extracellular contrast agent.

Enhancing capsule	CT	MRI	*P* value
Reader 1			
Overall	93 (93/210; 44.3%)	144 (144/210; 68.6%)	< **0.001**
HCC measuring < 30 mm	19 (19/66; 28.8%)	33 (33/66; 50.0%)	**0.004**
HCC measuring 30–49 mm	28 (28/59; 47.5%)	43 (43/59; 72.9%)	**0.001**
HCC measuring ≥ 50mm	46 (46/85; 54.1%)	68 (68/85: 80.0%)	< **0.001**
Reader 2			
Overall	100 (100/210; 47.6%)	151 (151/210; 71.9%)	< **0.001**
HCC measuring < 30 mm	22 (22/66; 33.3%)	42 (42/66; 63.6%)	< **0.001**
HCC measuring 30–49 mm	30 (30/59; 50.8%)	46 (46/59; 78.0%)	**0.001**
HCC measuring ≥ 50 mm	48 (48/85; 56.5%)	63 (63/85; 74.1%)	**0.001**
Inter-reader agreement (95% CI)	0.55 (0.4–0.66)	0.57 (0.45–0.70)	

Categorical variables are expressed as raw numbers; numbers in parentheses are proportions followed by percentages and were compared using McNemar test. Inter-reader agreement was assessed using Cohen kappa (*k*) test.
CI: confidence interval; CT: computed tomography; HCC: hepatocellular carcinoma; MRI: magnetic resonance imaging.
Bold indicates significant *P* value.

capsule (R1, 84.9% *vs.* 54.7%, $P < 0.001$%; R2, 83.0% *vs.* 50.9%, $P < 0.001$), which was observed in all tumor size subgroups. Overall, the accuracy of ECA-MRI was greater than that of contrast-enhanced CT (R1, 71.0% *vs.* 61.9%, $P = 0.032$; R2, 72.4% *vs.* 64.3%, $P = 0.060$). In HCCs with microscopic capsule only, enhancing capsule was visualized in 7/11 (63.6%, R1) and 6/11 (54.5%, R2) on ECA-MRI, while in 1/11 (9.1%, R1) and 3/11 (27.3%, R2) on contrast-enhanced CT. The diagnostic performances of contrast-enhanced CT and ECA-MRI in HCC with macroscopic capsule only are detailed in Supplementary Table 1.

The prevalence of enhancing capsule according to the background liver parenchyma is reported in Table 4. The prevalence of enhancing capsules did not significantly differ between patients with cirrhosis (F4) and those without (F0–F3) on either imaging modality. Enhancing capsule was significantly more frequent on CT for R1 in patients with F0–F2 than in F3–F4 ($P = 0.029$). For both readers, enhancing capsule was more frequently depicted on CT in patients with steatosis (R1, $P = 0.040$; R2, $P = 0.017$). Presence of steatosis did not influence the visualization of enhancing capsule on MRI.

3.4. Inter-reader agreement

The inter-reader agreement (Table 2) for enhancing capsule was moderate on both contrast-enhanced CT ($k = 0.55$) and ECA-MRI ($k = 0.57$). The inter-reader agreement for both CT and ECA-MRI was greater in patients with advanced fibrosis (*i.e.*, F3–F4) compared to those with none to moderate fibrosis (*i.e.*, F0–F2, Table 4).

3.5. Impact of enhancing capsule on LI-RADS categorization

A total of 106 patients (92 men and 14 women) with a mean age of 58.1 ± 13.4 [SD] years (age range: 21–79 years) with 106 HCCs

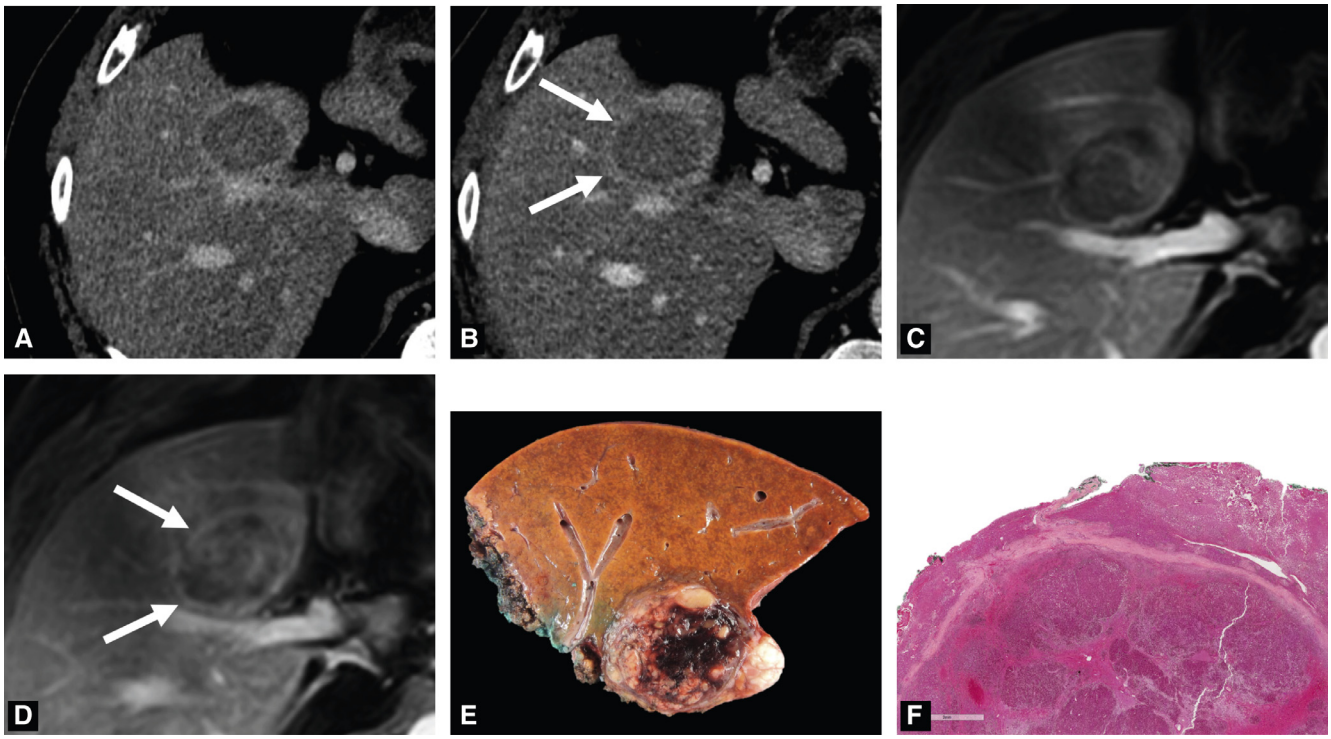

Fig. 2. 79-year-old man with chronic hepatitis B infection and 39-mm hepatocellular carcinoma located in segment V. Both readers agreed on the presence of enhancing capsule (arrows) on contrast-enhanced CT (A, portal venous phase; B, delayed phase) and on MRI with extracellular contrast agent (C, portal venous phase; D, delayed phase). After surgical resection, pathological specimens confirmed the presence of a fibrous capsule both macroscopically (E) and microscopically (F).

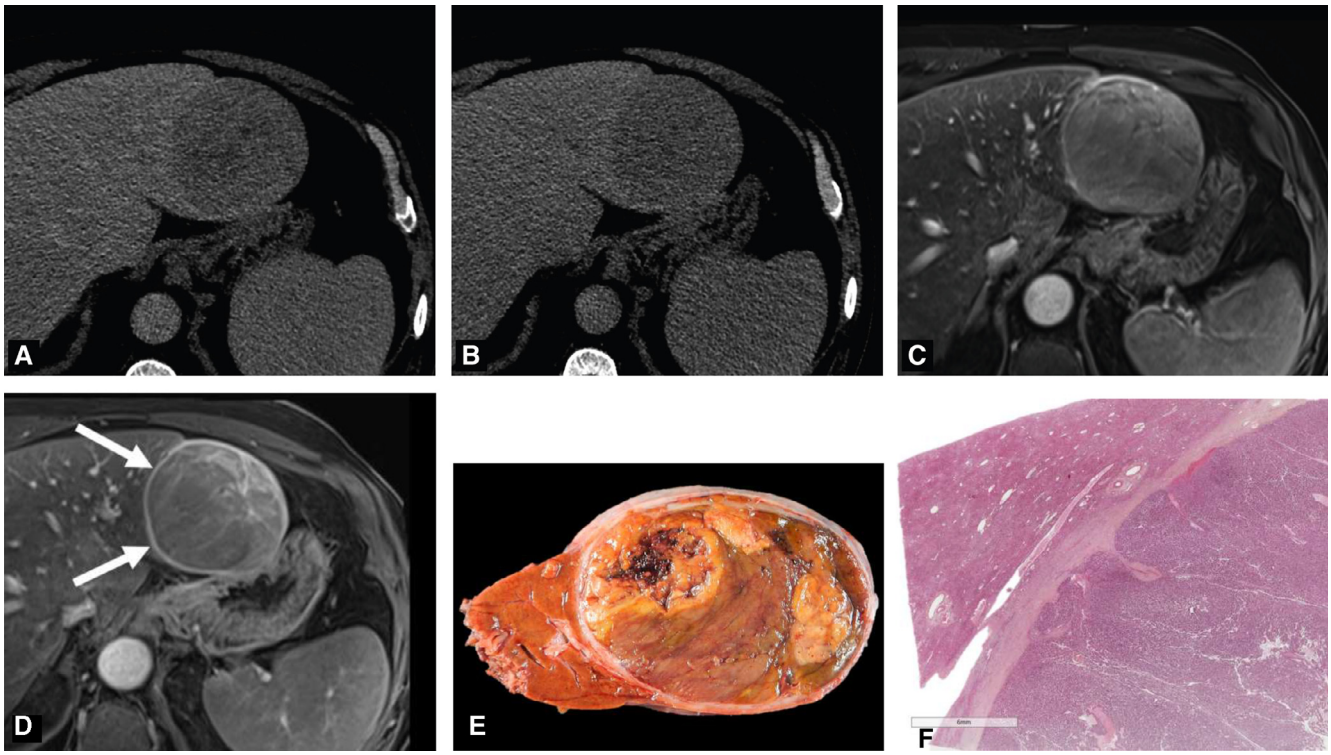

Fig. 3. 72-year-old man with nonalcoholic fatty liver disease and 86-mm hepatocellular carcinoma in the left lateral segment. Both readers agreed on the absence of enhancing capsule on contrast-enhanced CT (A, portal venous phase; B, delayed phase), while enhancing capsule (arrows) was observed by both readers on contrast-enhanced MRI (C, portal venous phase; D, delayed phase). After surgical resection, pathological specimens confirmed the presence of a fibrous capsule both macroscopically (E) and microscopically (F).

Table 3
Sensitivity, specificity, accuracy with true positive (TP), true negative (TN), false positive (FP), and false negative (FN) of enhancing capsule on contrast-enhanced CT and MRI with extracellular contrast agent for the diagnosis of capsule at histopathology.

Enhancing capsule	Sensitivity% (95% CI)	Specificity% (95% CI)	Accuracy% (95% CI)	TP	TN	FP	FN
All HCC (n = 210)							
CT							
Reader 1	54.1 (46.0–62.1) [85/157]	84.9 (72.4–93.2) [45/53]	61.9 (55.0–68.5) [130/210]	85	45	8	72
Reader 2	57.9 (49.8–65.8) [91/157]	83.0 (70.2–91.9) [44/53]	64.3 (57.4–70.8) [135/210]	91	44	9	66
MRI							
Reader 1	76.4 (69.0–82.8) [120/157]	54.7 (40.5–68.4) [29/53]	71.0 (64.3–77.0) [149/210]	120	29	24	37
Reader 2	79.6 (72.4–85.6) [125/157]	50.9 (36.8–64.9) [27/53]	72.4 (65.8–78.3) [152/210]	125	27	26	32
HCC < 30 mm (n = 66)							
CT							
Reader 1	36.6 (22.1–53.1) [15/41]	84.0 (63.9–95.4) [21/25]	54.6 (41.8–66.9) [36/66]	15	21	4	26
Reader 2	43.9 (28.5–60.2) [18/41]	84.0 (63.9–95.4) [21/25]	59.1 (46.3–71.1) [39/66]	18	21	4	23
MRI							
Reader 1	58.5 (42.1–73.7) [24/41]	64.0 (42.5–82.0) [16/25]	60.6 (47.8–72.4) [40/66]	24	16	9	17
Reader 2	73.2 (57.1–85.8) [30/41]	52.0 (31.3–72.2) [13/25]	65.2 (52.4–76.5) [43/66]	30	13	12	11
HCC 30–49 mm (n = 59)							
CT							
Reader 1	54.0 (39.3–68.1) [27/50]	88.9 (51.7–99.7) [8/9]	59.3 (45.8–71.9) [35/59]	27	8	1	23
Reader 2	58.0 (43.2–71.8) [29/50]	88.9 (51.7–99.7) [8/9]	62.7 (49.2–75.0) [37/59]	29	8	1	21
MRI							
Reader 1	76.0 (61.8–86.9) [38/50]	44.4 (13.7–78.8) [4/9]	71.2 (57.9–82.2) [42/59]	38	4	5	12
Reader 2	80.0 (66.3–90.0) [40/50]	33.3 (7.5–70.1) [3/9]	72.9 (59.7–83.6) [43/59]	40	3	6	10
HCC ≥ 50 mm (n = 85)							
CT							
Reader 1	65.2 (52.4–76.5) [43/66]	84.2 (60.4–96.6) [16/19]	69.4 (58.5–79.0) [59/85]	43	16	3	23
Reader 2	66.7 (54.0–77.8) [44/66]	78.9 (53.4–93.9) [15/19]	69.4 (58.5–79.0) [59/85]	44	15	4	22
MRI							
Reader 1	87.9 (77.5–94.6) [58/66]	47.4 (24.4–71.1) [9/19]	78.8 (68.6–86.9) [67/85]	58	9	10	8
Reader 2	83.3 (72.1–91.4) [55/66]	57.9 (33.5–79.7) [11/19]	77.6 (67.3–86.0) [66/85]	55	11	8	11

Data are expressed as percentages, data in parenthesis are 95% confidence intervals (95% CI), data in brackets are proportions.
Abbreviations. CI: confidence interval; CT: computed tomography; FN: false negative; FP: false positive; HCC: hepatocellular carcinoma; MRI: magnetic resonance imaging; TN: true negative; TP: true positive.

Table 4
Presence of tumor capsule on pathology and depiction of enhancing capsule on contrast-enhanced CT and MRI with extracellular contrast agent according to the quality of the background liver parenchyma.

	Background liver parenchyma F0–F3 (*n* = 142)	F4 (*n* = 68)	*P* value
Capsule on pathology			
Macro	102 (102/142; 71.8%)	44 (44/68; 64.7%)	0.294
Micro	109 (109/142; 76.8%)	48 (48/68; 70.6%)	0.335
Capsule at imaging			
CT			
Reader 1	66 (66/142; 46.5%)	27 (27/68; 39.7%)	0.355
Reader 2	73 (73/142; 48.6%)	31 (31/68; 45.6%)	0.683
Inter-reader agreement*	0.53 (0.39–0.67)	0.58 (0.39–0.67)	
MRI			
Reader 1	100 (100/142; 70.4%)	44 (44/68; 67.7%)	0.404
Reader 2	105 (105/142; 73.9%)	45 (45/68; 67.6%)	0.342
Inter-reader agreement*	0.56 (0.41–0.71)	0.61 (0.41–0.81)	
	F0–F2 (*n* = 93)	F3–F4 (*n* = 117)	
Capsule on pathology			
Macro	72 (72/93; 77.4%)	74 (74/117; 63.2%)	**0.027**
Micro	73 (73/93; 78.5%)	84 (84/117; 71.8%)	0.267
Capsule at imaging			
CT			
Reader 1	49 (49/93; 52.7%)	44 (44/117; 37.6%)	**0.029**
Reader 2	50 (50/93; 53.8%)	50 (50/117; 42.7%)	0.112
Inter-reader agreement*	0.46 (0.28–0.64)	0.61 (0.47–0.75)	
MRI			
Reader 1	70 (70/93; 75.3%)	74 (74/117; 63.2%)	0.062
Reader 2	71 (71/93; 76.3%)	80 (80/117; 68.4%)	0.202
Inter-reader agreement*	0.44 (0.23–0.65)	0.66 (0.52–0.80)	
	No steatosis (*n* = 127)	Steatosis (*n* = 83)	
Capsule on pathology			
Macro	90 (90/127; 70.9%)	56 (56/83; 67.5%)	0.601
Micro	95 (95/127; 74.8%)	62 (62/83; 74.7%)	0.986
Capsule at imaging			
CT			
Reader 1	49 (49/127; 38.6%)	44 (44/83; 53.0%)	**0.040**
Reader 2	52 (52/127; 40.9%)	48 (48/83; 57.8%)	**0.017**
Inter-reader agreement*	0.55 (0.40–0.70)	0.51 (0.32–0.69)	
MRI			
Reader 1	84 (84/127; 66.1%)	60 (60/86; 72.3%)	0.348
Reader 2	92 (92/127; 72.4%)	59 (59/83; 71.1%)	0.831
Inter-reader agreement	0.63 (0.48–0.77)	0.49 (0.28–0.70)	

Categorical variables are expressed as numbers and percentages and were compared using the Pearson $\chi 2$ or Fisher exact test. Bold indicates significant *P* value.
CT: computed tomography; MRI: magnetic resonance imaging.
* calculated using Cohen's kappa (*k*) test; numbers in parentheses are 95% confidence interval.

(mean size 42.8 ± 31.8 [SD] mm; range 9–159 mm) met the LI-RADS criteria for high-risk status. LI-RADS categories with and without enhancing capsule as a major feature are reported in Fig. 4. When the presence of a capsule was included as a major imaging feature on contrast-enhanced CT, six (5.6%) and three (2.8%) observations were upgraded by R1 (four were upgraded from LR-4 to LR-5; two from LR-3 to LR-4) and R2 (one upgraded from LR-4 to LR-5, two from LR-3 to LR-4), respectively. When the presence of a capsule was included as a major imaging feature on ECA-MRI, five (4.7%) and one (0.9%) observations were upgraded by R1 (two from LR-4 to LR-5; three from LR-3 to LR-4) and R2 (one from LR-4 to LR-5), respectively.

4. Discussion

This intraindividual comparative study demonstrates that enhancing capsule was significantly more frequently identified on ECA-MRI ECA than on contrast-enhanced CT, regardless of the size of HCC. The sensitivity of ECA-MRI was significantly greater while the specificity of CT was significantly greater with pathology as reference.

When enhancing capsule is integrated as a major imaging feature for the diagnosis of HCC in the LI-RADS algorithm it was shown to have a high specificity for the noninvasive diagnosis of HCC [5–8]. Because both contrast-enhanced CT and ECA-MRI are extensively used in clinical practice for the noninvasive diagnosis of HCC, the visualization of enhancing capsule might influence the categorization of a lesion as definitively HCC. Based on the LI-RADS v2018 algorithm, the presence of enhancing capsule allows the LR-5 categorization in observations with nonrim arterial phase hyperenhancement, measuring 10–19 mm and having another additional major feature, or in observations equal or larger than 20 mm, even in absence of other major features [9]. In our study, the final LI-RADS category was upgraded in 2.8–5.6% tumors on contrast-enhanced CT in the presence of enhancing capsule and in 0.9–4.7% lesions on ECA-MRI in the subset of patients with LI-RADS high-risk status.

Although several studies have compared different imaging features of HCC in different modalities and identified a similar rate of arterial phase hyperenhancement and washout on CT and ECA-MRI, only a few studies have assessed the intraindividual differences of imaging modalities for the visualization of enhancing capsule, with heterogeneous results [10–13,20–23]. In an intraindividual comparison of 216 HCCs, Joo et al. reported that enhancing capsule was significantly less frequent on gadoxetate disodium-enhanced MRI than on contrast-enhanced CT (17% *vs.* 31%) [10]. On the other hand, no

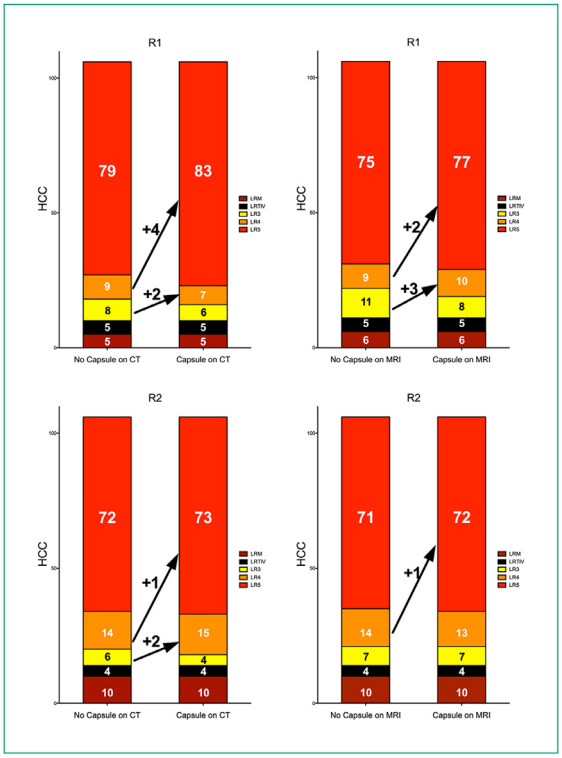

Fig. 4. LI-RADS category without and with enhancing capsule as major feature, in the LI-RADS v2018 high-risk population. HCC: hepatocellular carcinoma R: reader.

difference was observed in the visualization of enhancing capsule on gadoxetate disodium-enhanced MRI and contrast-enhanced CT (30.0% *vs* 30.5%) in a multicenter intraindividual study by An et al. including 231 hepatic lesions (114 HCCs) [23]. Song et al. showed that capsule was more common on MRI with gadopentetate dimeglumine than with gadoxetate disodium (75% *vs* 50%) in an intraindividual comparison of 77 HCCs [12]. In a prospective intraindividual comparison of 117 lesions, Min et al. more frequently identified enhancing capsule with ECA than gadoxetate disodium MRI (87% *vs* 47%) [13]. The less frequent visualization of the enhancing capsule on gadoxetate disodium-enhanced MRI in these studies could be because the appearance of the capsule may be hidden by the increasing signal intensity of the liver during the transitional phase [24]. It is interesting to note that in our study there was a greater frequency of enhancing capsules than in prior reports (44–47% on contrast-enhanced CT and 68–72% on ECA-MRI), probably due to the larger HCC tumors (mean size, 56 mm) and to the greater prevalence of HCC capsules on histopathology in lesions ≥ 30 mm in our cohort.

Moreover, our study evaluated the performance of contrast-enhanced CT and ECA-MRI using histopathology as the reference. Overall, the accuracy of ECA-MRI was slightly higher than contrast-enhanced CT (71–72% *vs.* 62–64%). Interestingly, the sensitivity of ECA-MRI was significantly better than contrast-enhanced CT for the diagnosis of tumor capsules (76–79% *vs.* 54–58%), while contrast-enhanced CT had a significantly higher specificity than ECA-MRI for tumor capsule (83–85% *vs* 51–55%). The increased sensitivity of MRI may be due to better contrast resolution with this technique. The lower specificity of ECA-MRI may be related to a better visualization of the compressed liver parenchyma adjacent to the lesions (depicted as pseudocapsule on imaging), mimicking the presence of a true perilesional enhancing capsule but without peritumoral fibrous capsule at pathology [25]. The difference between capsule and pseudocapsule cannot be made by imaging. However, this difference is not relevant for the noninvasive diagnosis of HCC and for the prediction of histopathological aggressiveness [25].

The sensitivity of CT in our study was lower than that reported by Kim et al. [26]. In that study, the sensitivity and specificity of CT and gadoxetate disodium MRI were similar (CT, 71%; MRI, 73%; and CT, 76%; MRI, 70%, respectively) for the diagnosis of a histopathological capsule in 63 HCCs [26]. Of note, in our study the presence of underlying cirrhosis did not significantly influence the visualization of an enhancing capsule in either imaging technique, while enhancing capsule was more frequently depicted on CT in patient with hepatic steatosis. This could be explained by the more hypoattenuating appearance of the steatotic liver.

Inter-reader agreement for the presence of enhancing capsule in our study was moderate on both contrast-enhanced CT (*k*: 0.55) and ECA-MRI (*k*: 0.57), which is in accordance with previous studies (*k* range: 0.42–0.88) [27–29]. In a recent meta-analysis [30], the inter-reader agreement for enhancing capsule on MRI (meta-analytic pooled *k*: 0.66) was similar to other major imaging features (meta-analytic pooled *k* range: 0.69–0.72) for the diagnosis of HCC, although substantial heterogeneity was noted across studies. Interestingly, in our cohort, inter-reader agreement was better in patients with advanced fibrosis (F3–F4) despite similar rate of tumor capsule on pathological analysis. This may be due to a better depiction of the capsule in these patients.

Our retrospective study has several limitations. First, the inclusion of only pathologically-proven HCCs after hepatic resection with both pretreatment CT and MRI could create a selection bias. Moreover, most HCCs in our cohort were larger than 30 mm, and 40% were larger than 50 mm, which could limit the applicability of the results to smaller lesions and influence the value of enhancing capsule for LI-RADS categorization in patients at high risk of HCC. Second, our study cohort included patients with different etiologies of chronic liver disease, and a pathological diagnosis of cirrhosis in only one third of patients. A lack of cirrhosis or a high-risk status for HCC requires diagnostic confirmation by biopsy even in the presence of typical imaging features of HCC [1,31]. Third, our study did not include a control group with non-HCC lesions, limiting the assessment of the sensitivity and specificity of enhancing capsule for the differential diagnosis of HCCs with other benign lesions and non-HCC malignancies. Finally, we did not evaluate the presence of a non-enhancing capsule, which is currently listed as an ancillary feature favoring malignancy in the LI-RADS algorithm [9]. Nevertheless, this feature is rarely observed on CT or MRI [13,29].

In conclusion, enhancing capsule was more frequently visualized on ECA-MRI than on contrast-enhanced CT. ECA-MRI was significantly more sensitive for the diagnosis of an HCC capsule, while the specificity of contrast-enhanced CT was better, regardless of tumor size.

Author contributions

All authors attest that they meet the current International Committee of Medical Journal Editors (ICMJE) criteria for Authorship.

Disclosure of Interests

The authors declare that they have no competing interest.

Human rights

The authors declare that the work described has been carried out in accordance with the Declaration of Helsinki of the World Medical Association revised in 2013 for experiments involving humans.

Informed consent and patient details

The authors declare that this report does not contain any personal information that could lead to the identification of the patients.

CRediT authorship contribution statement

Roberto Cannella: Conceptualization, Methodology, Formal analysis, Investigation, Data curation, Writing – original draft. **Maxime Ronot:** Conceptualization, Methodology, Formal analysis, Writing – review & editing, Supervision. **Riccardo Sartoris:** Data curation, Writing – review & editing. **Francois Cauchy:** Investigation, Writing – review & editing. **Christian Hobeika:** Investigation, Data curation, Writing – review & editing. **Aurélie Beaufrere:** Investigation, Writing – review & editing. **Loïc Trapani:** Investigation, Writing – review & editing. **Valérie Paradis:** Investigation, Writing – review & editing. **Mohamed Bouattour:** Data curation, Writing – review & editing. **Fanny Bonvalet:** Writing – review & editing. **Valérie Vilgrain:** Conceptualization, Writing – review & editing, Supervision. **Marco Dioguardi Burgio:** Conceptualization, Methodology, Formal analysis, Investigation, Data curation, Writing – original draft, Writing – review & editing, Supervision.

Funding

This work did not receive any grant from funding agencies in the public, commercial, or not-for-profit sectors.

Supplementary materials

Supplementary material associated with this article can be found, in the online version, at doi:10.1016/j.diii.2021.06.004.

References

[1] European Association for the Study of the Liver. EASL clinical practice guidelines: management of hepatocellular carcinoma. J Hepatol 2018;69:182–236.
[2] Choi JY, Lee JM, Sirlin CB. CT and MR imaging diagnosis and staging of hepatocellular carcinoma: part I. Development, growth, and spread: key pathologic and imaging aspects. Radiology 2014;272:635–54.
[3] Choi BI, Lee JM, Kim TK, Dioguardi Burgio M, Vilgrain V. Diagnosing borderline hepatic nodules in hepatocarcinogenesis: imaging performance. AJR Am J Roentgenol 2015;205:10–21.
[4] Tang A, Bashir MR, Corwin MT, Cruite I, Dietrich CF, Do RKG, et al. LI-RADS Evidence Working Group. Evidence supporting LI-RADS major features for CT- and MR imaging-based diagnosis of hepatocellular carcinoma: a systematic review. Radiology 2018;286:29–48.
[5] Cerny M, Bergeron C, Billiard JS, Murphy-Lavallée J, Olivié D, Bérubé J, et al. LI-RADS for MR imaging diagnosis of hepatocellular carcinoma: performance of major and ancillary features. Radiology 2018;288:118–28.
[6] Kim YY, Kim MJ, Kim EH, Roh YH, An C. Hepatocellular carcinoma *versus* other hepatic malignancy in cirrhosis: performance of LI-RADS version 2018. Radiology 2019;291:72–80.
[7] Vernuccio F, Cannella R, Meyer M, Choudhoury KR, Gonzáles F, Schwartz FR, et al. LI-RADS: diagnostic performance of hepatobiliary phase hypointensity and major imaging features of LR-3 and LR-4 lesions measuring 10–19 mm with arterial phase hyperenhancement. AJR Am J Roentgenol 2019;213:W57–65.
[8] Shin J, Lee S, Yoon JK, Chung YE, Choi JY, Park MS. LI-RADS Major features on MRI for diagnosing hepatocellular carcinoma: a systematic review and meta-analysis. J Magn Reson Imaging 2021. doi: 10.1002/jmri.27570.
[9] American College of Radiology. CT/MRI liver imaging reporting and data system v2018 core. https://www.acr.org/Clinical-Resources/Reporting-and-Data-Systems/LI-RADS/CT-MRI-LI-RADS-v2018 Accessed April 2021.
[10] Joo I, Lee JM, Lee DH, Ahn SJ, Lee ES, Han JK. Liver imaging reporting and data system v2014 categorization of hepatocellular carcinoma on gadoxetic acid-enhanced MRI: comparison with multiphasic multidetector computed tomography. J Magn Reson Imaging 2017;45:731–40.
[11] Dioguardi Burgio M, Picone D, Cabibbo G, Midiri M, Lagalla R, Brancatelli G. MR-imaging features of hepatocellular carcinoma capsule appearance in cirrhotic liver: comparison of gadoxetic acid and gadobenate dimeglumine. Abdom Radiol 2016;41:1546–54.
[12] Allen BC, Ho LM, Jaffe TA, Miller CM, Mazurowski MA, Bashir MR. Comparison of visualization rates of LI-RADS version 2014 major features with iv gadobenate dimeglumine or gadoxetate disodium in patients at risk for hepatocellular carcinoma. AJR Am J Roentgenol 2018;210:1266–72.
[13] Paisant A, Vilgrain V, Riou J, Oberti F, Sutter O, Laurent V, et al. Comparison of extracellular and hepatobiliary MR contrast agents for the diagnosis of small HCCs. J Hepatol 2020;72:937–45.
[14] Song JS, Choi EJ, Hwang SB, Hwang HP, Choi H. LI-RADS v2014 categorization of hepatocellular carcinoma: intraindividual comparison between gadopentetate dimeglumine-enhanced MRI and gadoxetic acid-enhanced MRI. Eur Radiol 2019;29:401–10.
[15] Min JH, Kim JM, Kim YK, Kang TW, Lee SJ, Choi GS, et al. Prospective intraindividual comparison of magnetic resonance imaging with gadoxetic acid and extracellular contrast for diagnosis of hepatocellular carcinomas using the Liver Imaging Reporting and Data System. Hepatology 2018;68:2254–66.
[16] Cheng Z, Yang P, Qu S, Zhou J, Yang J, Yang X, Xia Y, Li J, Wang K, Yan Z, Wu D, Zhang B, Hüser N, Shen F. Risk factors and management for early and late intrahepatic recurrence of solitary hepatocellular carcinoma after curative resection. HPB 2015;17:422–7.
[17] Lee EC, Kim SH, Park H, Lee SD, Lee SA, Park SJ. Survival analysis after liver resection for hepatocellular carcinoma: a consecutive cohort of 1002 patients. J Gastroenterol Hepatol 2017;32:1055–63.
[18] Bedossa P, Poynard T. An algorithm for the grading of activity in chronic hepatitis C. The METAVIR Cooperative Study Group. Hepatology 1996;24:289–93.
[19] Benchoufi M, Matzner-Lober E, Molinari N, Jannot AS, Soyer P. Interobserver agreement issues in radiology. Diagn Interv Imaging 2020;101:639–41.
[20] Ding Y, Rao SX, Wang WT, Chen CZ, Li RC, Zeng M. Comparison of gadoxetic acid *versus* gadopentetate dimeglumine for the detection of hepatocellular carcinoma at 1.5 T using the liver imaging reporting and data system (LI-RADS v.2017). Cancer Imaging 2018;18:48.
[21] Kim YN, Song JS, Moon WS, Hwang HP, Kim YK. Intra-individual comparison of hepatocellular carcinoma imaging features on contrast-enhanced computed tomography, gadopentetate dimeglumine-enhanced MRI, and gadoxetic acid-enhanced MRI. Acta Radiol 2018;59:639–48.
[22] Nakao S, Tanabe M, Okada M, Furukawa M, Iida E, Miyoshi K, et al. Liver imaging reporting and data system (LI-RADS) v2018: comparison between computed tomography and gadoxetic acid-enhanced magnetic resonance imaging. Jpn J Radiol 2019;37:651–9.
[23] An C, Lee CH, Byun JH, Lee MH, Jeong WK, Choi SH, et al. Intraindividual comparison between gadoxetate-enhanced magnetic resonance imaging and dynamic computed tomography for characterizing focal hepatic lesions: a multicenter, multireader study. Korean J Radiol 2019;20:1616–26.
[24] Dioguardi Burgio M, Ronot M, Paulatto L, Terraz S, Vilgrain V, Brancatelli G. Avoiding pitfalls in the interpretation of gadoxetic acid-enhanced magnetic resonance imaging. Semin Ultrasound CT MR 2016;37:561–72.
[25] Ishigami K, Yoshimitsu K, Nishihara Y, Irie H, Asayama Y, Tajima T, et al. Hepatocellular carcinoma with a pseudocapsule on gadolinium-enhanced MR images: correlation with histopathologic findings. Radiology 2009;250:435–43.
[26] Kim B, Lee JH, Kim JK, Kim HJ, Kim YB, Lee D. The capsule appearance of hepatocellular carcinoma in gadoxetic acid-enhanced MR imaging: correlation with pathology and dynamic CT. Medicine 2018;97:e11142.
[27] Ehman EC, Behr SC, Umetsu SE, Fidelman N, Yeh BM, Ferrell LD, Hope TA. Rate of observation and inter-observer agreement for LI-RADS major features at CT and MRI in 184 pathology proven hepatocellular carcinomas. Abdom Radiol 2016;41:963–9.
[28] Fowler KJ, Tang A, Santillan C, Bhargavan-Chatfield M, Heiken J, Jha RC, et al. Interreader Reliability of LI-RADS version 2014 algorithm and imaging features for diagnosis of hepatocellular carcinoma: a large international multireader study. Radiology 2018;286:173–85.
[29] Ludwig DR, Fraum TJ, Cannella R, Ballard DH, Tsai R, Naeem M, LeBlanc M, Salter A, Tsung A, Shetty AS, Borhani AA, Furlan A, Fowler KJ. Hepatocellular carcinoma (HCC) *versus* non-HCC: accuracy and reliability of Liver Imaging Reporting and Data System v2018. Abdom Radiol 2019;44:2116–32.
[30] Kang JH, Choi SH, Lee JS, Park SH, Kim KW, Kim SY, Lee SS, Byun JH. Interreader agreement of liver imaging reporting and data system on MRI: a systematic review and meta-analysis. J Magn Reson Imaging 2020;52:795–804.
[31] Mamone G, Di Piazza A, Carollo V, Crinò F, Vella S, Cortis K, et al. Imaging of primary malignant tumors in non-cirrhotic liver. Diagn Interv Imaging 2020;101:519–35.